NIPPON STEEL TECHNICAL REPORT No. 91 January 2005

UDC 620 . 186 . 1 : 620 . 187

Visualization of Nano-precipitate in Low-alloy Steel by Using Energy-filtered Transmission Electron Microscopy

Yoichi IKEMATSU*1 Genichi SHIGESATO*1
Masaaki SUGIYAMA*1

Abstract

Based on the priniple of energy-filtered transmission electron microscopy (EF-TEM), characterization technique for the elemental distribution on local area in materials are discussed. The study for visualization of nano-precipitates in a low-alloy steel including a small amount of titanium by using EF-TEM has been also introduced. Through the study, it was clarified that the measurement of elemental distribution using EF-TEM is quite useful to visualize nano-precipitates containing transition metals such as titanium in low-alloy steels.

1. Introduction

Fine precipitates and non-metallic inclusions play important roles in the formation of the microstructure of low-alloy steels. For example, they are used not only for precipitation strengthening but also as the nucleation sites of the intra-granular ferrite in the heat-affected zones of welded joints to refine the microstructure and as the pinning particles to suppress the grain growth. Fine precipitates more than 100 nm in size were used for the above purposes, however ultra-fine precipitates up to tens of nanometers in size, called nano-precipitates, have recently come to be used to control the microstructure. As a consequence, the importance of the characterization of these precipitates has increased.

Transmission electron microscopes (TEMs) have been used for the analysis of the microstructure of steel; they constitute a powerful tool especially for analyzing the shape and crystal structure of nano-precipitates in steel[1]. Furthermore, with a field-emission transmission electron microscope (FE-TEM), which is equipped with a field-emission type electron gun, it is possible to use a high-intensity, high-coherence electron beam. In combination with an analysis system of energy-dispersive X-ray spectroscopy (EDS) or electron energy-loss spectroscopy (EELS), FE-TEM is capable of analyzing the composition of a nano-precipitate[2, 3].

EDS produces an element distribution image that shows the distribution of elements by analyzing the characteristic X-rays emitted from a point to be analyzed. However, the measurement of elemental analysis by EDS takes a long time because the object for observation must be scanned with an electron beam. What is more, owing to the limited detection sensitivity of EDS, it is often difficult to measure the distribution of so-called light elements such as C and N, which are important in the composition analysis of fine precipitates in steel using this method. On the other hand, EELS is capable of measuring the distribution of C and N, because the sensitivity of the method for light elements is high[4].

Recently, TEMs equipped with a high-performance energy filter (energy-filtered TEMs) are being used to analyze the microstructure of various advanced materials[4, 5]. An energy-filtered TEM is based on the EELS system for analyzing the chemical composition and bonding state of materials, by measuring the amount of energy-loss of incident electrons as a result of their interaction with the specimen as they pass therethrough. With an energy-filtered TEM, it is possible not only to measure the energy-loss spectrum of electrons, but also to produce an image of the microstructure of a specimen by choosing electrons having a specific amount of energy from among those that undergo energy spectrometry. For this reason, it is presumed possible with an energy-filtered TEM to visualize a nano-precipitate in steel as small as tens of nanometers in size by forming an element distribution image of the precipitate. Thus the device is expected to enable us to observe the distribution of nano-precipi-

*1 Advanced Technology Research Laboratories

tates, the observation of which is indispensable in the study of fine precipitates in low-alloy steels.

This paper describes a study on the visualization of nano-precipitates in a low-alloy steel using an energy-filtered TEM. The paper also discusses the effectiveness of an energy-filtered TEM in the analysis of nano-precipitates in low-alloy steels, based on the results of the visualization.

2. Outline of Energy-filtered TEM[6)]

The energy filters developed recently for general TEMs are broadly classified into two types (see **Fig. 1**). One is the in-column type to be installed in the lens of a TEM; the energy spectrometers of the omega type[7)], Castaing-Henry type[8)] and the like, fall within this category. The other is the post-column type to be installed in the bottom of the camera chamber of a TEM; the widely used sector type energy spectrometers fall into this category[9)]. Either type can form electron microscope images and electron diffraction patterns by using the selected electrons that have lost a specified amount of energy using a slit provided for that purpose. Whereas the in-column type can use either an imaging plate or a slow-scanning CCD camera as a recording medium, the post-column type uses exclusively a slow-scanning CCD camera. Although there are some differences between the two types optically, the basic principles are the same.

Here, the outline of an energy-filtered TEM is explained based on the TEM equipped with an in-column type energy filter that was employed for the authors' analysis.

Fig. 2 is a schematic sectional view showing the basic configuration of the TEM equipped with an omega-type energy filter used for the present study. The omega-type energy filter, which is provided inside the TEM proper between the intermediate and the projector lenses, analyzes the energy spectrum of electrons that have passed through a specimen using four sector-shaped magnets. This type of energy filter is called the omega type because an electron beam is bent into a curve having the shape of the Greek letter Ω.

Fig. 3(a) is a schematic illustration showing the energy dispersion in an omega-type energy filter. Electrons having passed through a specimen go through objective and intermediate lenses, and then are introduced into the energy filter. Each of the four magnets of the energy filter generates a homogeneous magnetic field, and the magnetic field bends the trajectories of the electrons depending on their velocity to disperse their energy. The electrons undergo intensive energy dispersion especially at the fourth magnet, and as a result, an electron energy-loss spectrum as shown in Fig. 3(b) forms at a downstream position.

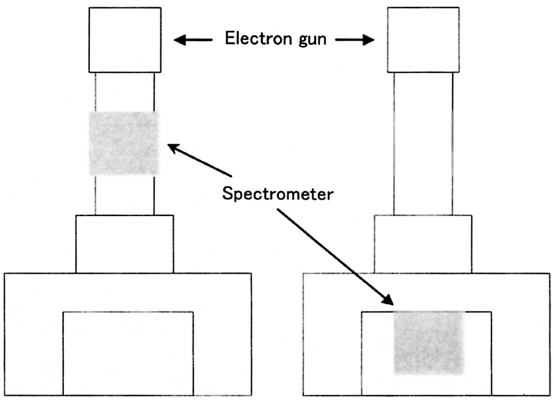

(a) In-column type **(b) Post-column type**

Fig. 1 Schematic illustrations of two types of energy-filtered TEMs

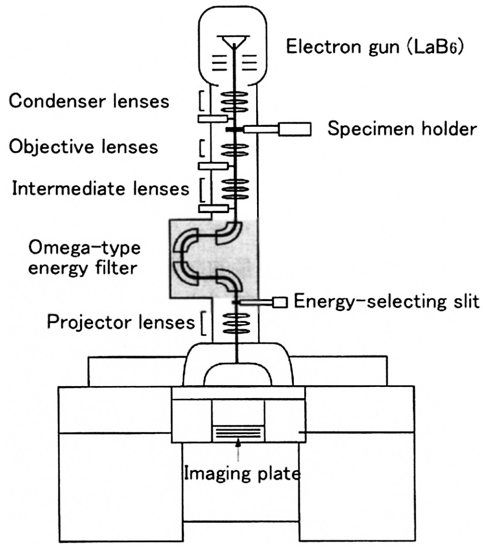

Fig. 2 Configuration of omega-type energy-filtered TEM

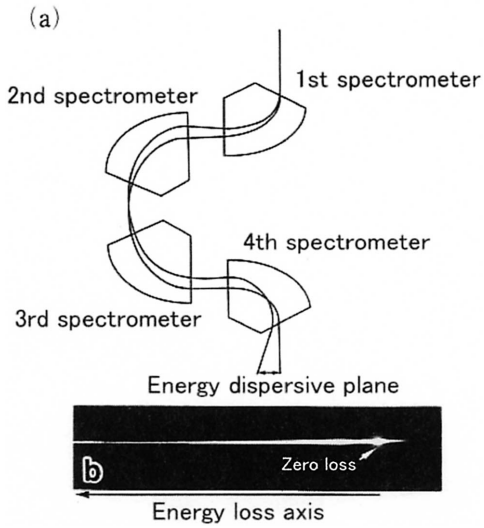

Fig. 3 Schematic illustration of energy dispersion by omega-type energy filter (a) and electron energy-loss spectrum (b)

Because the omega-type energy filter is a double-convergence type spectrometer, the electron energy-loss spectrum that forms has a shape as shown in Fig. 3(b). An energy selective slit is provided at the plane where the electron energy-loss spectrum forms. After the observation of an electron energy-loss spectrum, electrons possessing a given amount of energy are selected from the spectrum by inserting the energy-selecting slit, and through image formation using the selected electrons, an energy-filtered image is obtained. The energy selective slit is structured so that its width and position are changeable according to the purpose of observation; usually, an energy-filtered image is formed setting the slit width at the value corresponding to 10 to 30 eV.

For further details of the omega-type energy filter used for the present study, see reference literature 4).

3. Experimental Procedure

A low-alloy steel (Fe-0.12 mass % C-1.4 mass % Mn) containing a small amount of Ti and prepared in a vacuum melting furnace was rolled, and a 15 mm × 15 mm × 10 mm block specimen was cut out from the rolled steel. The block specimen was machine polished and buffed to a mirror surface, then that surface was etched by the SPEED method, which is an etching method by controlled potential electrolysis using an electrolyte of a non-aqueous solvent. The etched specimen was then washed by ethanol solution and left to dry naturally. From the surface thus prepared, precipitates of TiN were extracted by the blank -replica method. TiN was selected as the object of the study because it is one of the precipitates widely used for controlling the microstructure of low-alloy steels.

The nano-precipitate of TiN was observed using the following equipment: a transmission electron microscope equipped with an omega-type energy filter (JEM-2010Ω[10] made by JEOL, accelerating voltage 200 kV) of Institute of Multidisciplinary Research for Advanced Materials, Tohoku University; and a transmission electron microscope (HF-2000 made by Hitachi Ltd., accelerating voltage 200 kV, with a field-emission type electron gun) equipped with a post-column type energy filter (Gatan Imaging Filter Model 678 made by Gatan). As quantitative recording media for TEM images, imaging plates (FDL-UR-V, pixel size 25 μm × 25 μm made by Fuji Photo Film Co., Ltd.), were used for the TEM equipped with the omega-type energy filter, and a slow-scanning CCD camera was applied for the TEM equipped with the post-column type energy filter.

4. Results and Discussion

Photo 1 is a bright-field image of the TiN precipitates on a carbon film, extracted from the low-alloy steel specimen by the replica method. Nano-precipitates tens of nanometers in size are observed. An EDS analysis revealed the peaks of nitrogen and titanium in the spectrum, and thus the precipitates were confirmed to be of TiN.

Photo 2(a) is an electron energy-loss spectrum obtained from the TiN nano-precipitates observed. Besides the strong zero-loss peak of elastically scattered electrons and transmission electrons, thin band of inelastically scattered electrons were observed in the spectrum. By a detailed examination of the bands revealed portions, such as that indicated as A in Photo 2(a), where signal intensity was slightly higher than the other portions. Photo 2(b) shows the signal intensity

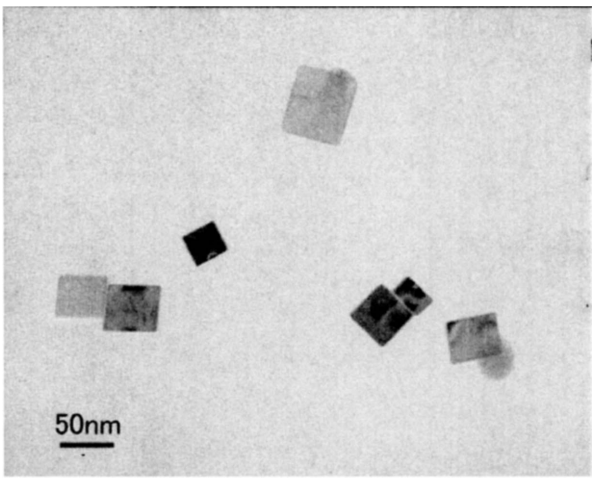

Photo 1 Bright-field image of nano-precipitates in a low-alloy steel extracted by replica method

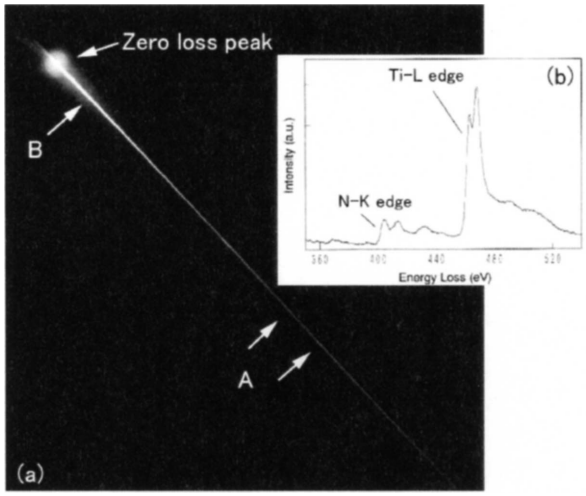

Photo 2 Electron energy-loss spectrum (a) obtained from a nano-precipitate, and intensity profile (b) of a part of the spectrum indicated by letter A

profile in portion A; there are rises in signal intensity called “edges” at 402 and 455 eV. From the energy-loss values at these edges, they were found to correspond to the K edge of nitrogen (N-K edge) and the L edge of titanium (Ti-L edge), respectively. Following the finding, energy-filtered images were observed at near the N-K and Ti-L edges.

In **Photo 3**, part (a) is an energy-filtered image of TiN that was produced using electrons that form the zero-loss peak, and parts (b) to (e) are the energy-filtered images obtained at near the N-K and Ti-L edges. The width of the energy -selecting slit used for forming the images is set to 20 eV. A pre-edge image is an energy-filtered image that is formed using inelastically scattered electrons in a region at the front of an edge, and a post-edge image is another formed using inelastically scattered electrons that form the edge. In these energy-filtered images, the TiN precipitate shows itself in clear contrast to the support carbon film. Furthermore, comparing the pre-edge and post-edge images at the Ti-L edge, one sees TiN in a clearer contrast in the post-edge image than in the pre-edge one.

After the above, the authors formed jump-ratio images from the pre-edge and post-edge images. A jump-ratio image is an image obtained from a pre-edge and a post-edge image through the following calculation for each of the pixels:

$$I_s(x, y) = I_{post}(x, y) / I_{pre}(x, y) \quad (1)$$

where $I_s(x, y)$ is the signal intensity of each pixel of a jump-ratio image, $I_{post}(x, y)$ is the signal intensity of each pixel of a post-edge image and $I_{pre}(x, y)$ is the same of the corresponding pixel of a pre-edge image. **Photo 4** shows jump-ratio images of TiN obtained through the above image processing; it is seen here that TiN is clearly visualized as composition information indicating that it is composed of nitrogen, which is a light element, and titanium.

Next, the authors studied a method of visualizing TiN using edges of comparatively higher signal intensity existing on the lower energy-loss side to the N-K edge (402 eV) and the Ti-L edge (455 eV). **Fig. 4** is a signal intensity profile in the region indicated as B near the zero-loss peak of the electron energy-loss spectrum shown in Photo 2(a). Near the zero-loss peak of a very large intensity, there is a plasmon-loss peak formed by inelastically scattered electrons that have lost their energy as a result of plasmon excitation. Besides the

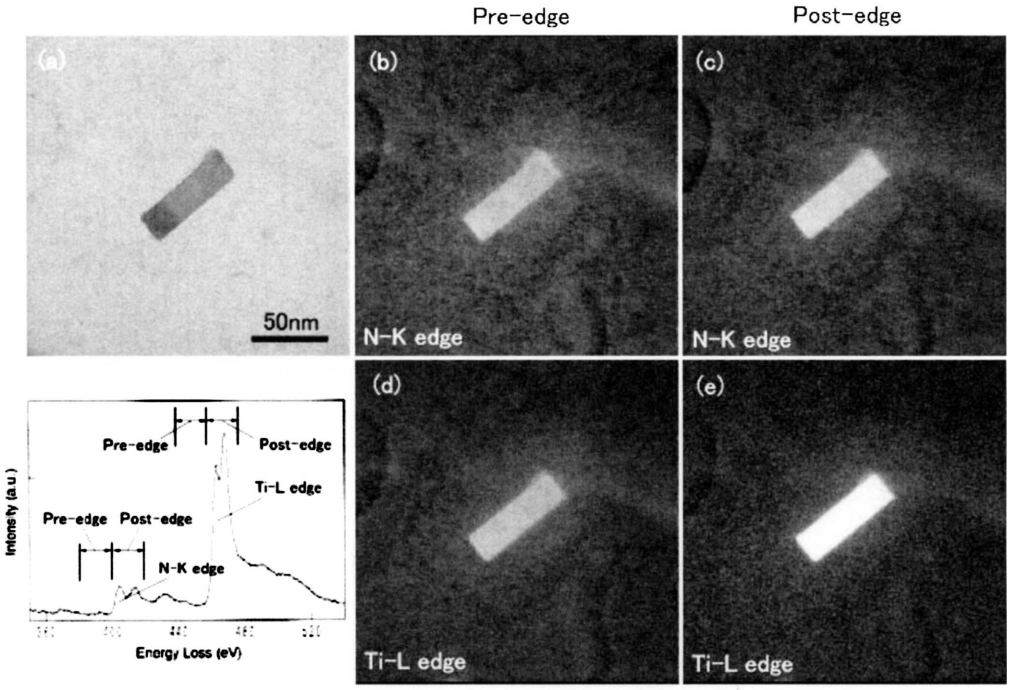

Photo 3 Energy-filtered images of a TiN observed at around N-K edge and Ti-L edge
(a) Zero-loss image, (b) Pre-edge image at N-K edge, (c) Post-edge image at N-K edge, (d) Pre-edge image at Ti-L edge, (e) Post-edge image at Ti-L edge

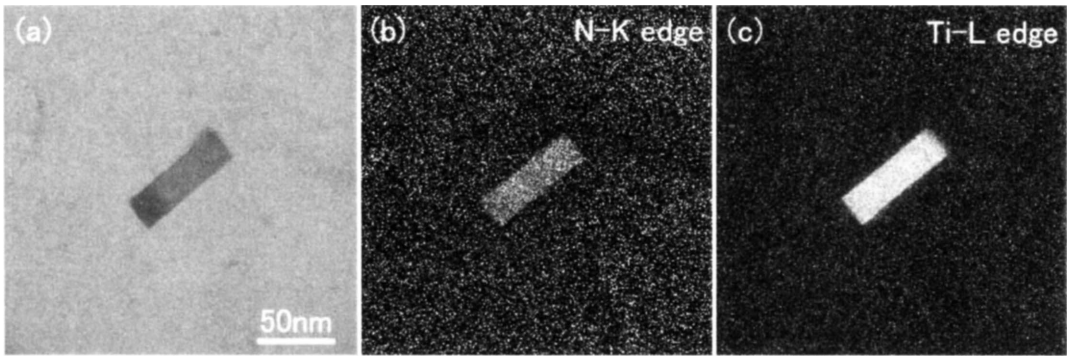

Photo 4 Zero-loss image (a) and jump-ratio images of TiN ((b) N-K edge, (c) Ti-L edge)

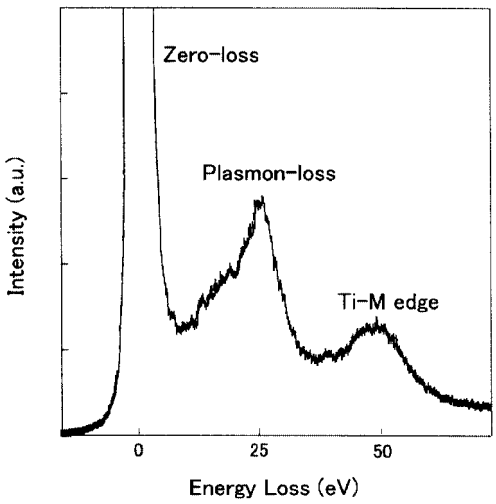

Fig. 4 Intensity profile of low-loss region in electron energy loss spectrum of TiN

plasmon-loss peak, there is another distinct edge at near 50 eV. From the value of its energy loss, this peak at near 50 eV is that of the M edge of titanium (Ti-M edge).

Photo 5 is an energy-filtered image obtained by setting the energy -selecting slit at the position of the Ti-M edge; TiN were clearly observed. As mention above, it is possible to obtain an energy-filtered image like the one shown in Photo 5 using the N-K edge (402 eV) or the Ti-L edge (455 eV), which are on the larger energy-loss side to the Ti-M edge. However, since the signal intensity is so low at these edges (lower than that at the Ti-M edge by two orders of magnitude) that the contrast of the energy-filtered images is very unclear at these edges, especially when a specimen is thick. For this reason, the image forming method using the Ti-M edge, which shows TiN in a clearer contrast, is better for analyzing a comparatively thick specimen or a nano-precipitate in a thin film specimen.

Photo 6 is an energy-filtered image formed using the Ti-M edge, visualizing the same TiN precipitates shown in Photo 1. From this image, it is clear that the visualization of nano-precipitates using the Ti-M edge is very effective in analyzing the distribution of TiN pre-

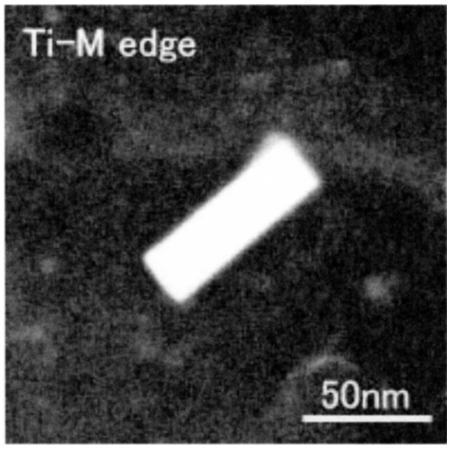

Photo 5 Energy-filtered image of TiN using Ti-M edge

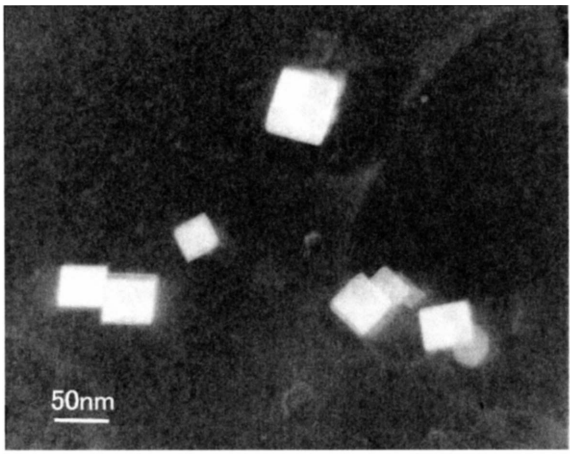

Photo 6 Energy-filtered image formed using Ti-M edge showing the same field of view shown in Photo 1

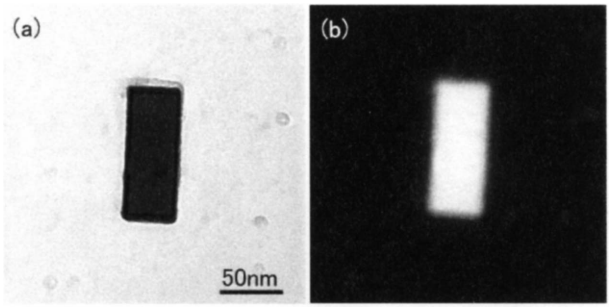

Photo 7 Energy-filtered image of TiN obtained by post-column type energy-filter
(a) Zero-loss image, (b) Energy-filtered image using Ti-M edge

cipitates.

Photo 7 is an energy-filtered image of TiN formed at the Ti-M edge using the TEM equipped with a post-column type energy filter. Here, TiN appears as clearly as in the energy-filtered image of Photo 6 obtained using the in-column type energy filter, and thus it is clear that the image forming using the Ti-M edge is effective also with a TEM equipped with a post-column type energy filter, which is more versatile than the in-column type.

Table 1 Inner-shell energies for M-shell of typical transition metals[11)]

Atomic number	22	23	24	25	26	27	28	29
Element	Ti	V	Cr	Mn	Fe	Co	Ni	Cu
Energy (eV)	47	47	48	51	57	62	68	74

Table 1[11)] shows the values of the inner-shell energy of the M shell, which corresponds to the energy loss at the M edge, of typical transition metal elements that form nano-precipitates in low-alloy steels. The table states that the energy loss at the M edge of Ti that composes TiN is 47 eV. The table also shows that besides Ti, other transition metal elements such as V and Cr have their M edges in a range of energy loss from 40 to 80 eV. Therefore, it is presumed possible to visualize nano-precipitates containing these transition metals by properly selecting the position and width of an energy-selecting slit.

5. Summary

This paper outlined the characteristics of an energy-filtered TEM that is capable of measuring the local elemental distribution of a material, and the principles of the measurement. Using such an energy-filtered TEM, the authors carried out visualization of nano-precipitates in a low-alloy steel containing a small amount of Ti. As a result, TiN precipitates as small as tens of nanometers in size were clearly visualized by forming an image using the M edge of Ti in the electron energy-loss spectrum that was obtained from a TiN precipitate in a low-alloy steel. The study demonstrated that the technique of visualizing nano-precipitates using an energy-filtered TEM was effective in the analysis of nano-precipitates essential for low alloy steels and the understanding of their distribution. Removing the background caused by the inelastic scattering of electrons will improve the quality of high-resolution images and electron diffraction patterns. Thus, applications of this technique is expected to expand to the detail analysis of the structure of nano-precipitates.

Acknowledgement

The authors express their sincere gratitude to Prof. Daisuke Shindo of Institute of Multidisciplinary Research for Advanced Materials, Tohoku University, for having facilitated the authors' use of the omega-type energy-filtered TEM of the laboratory and valuable advice on the observation data obtained.

References

1) Hirsch, P. B. et al.: Electron Microscopy of Thin Crystals. Butterworths, London, 1965, p.1
2) Maruyama, N., Uemori, R., Morikawa, H.: Shinnittetsu Giho. (359), 6(1996)
3) Sugiyama, M.: Materials Science and Technology. 40(5), 232(2003)
4) Shindo, D., Oikawa, T.: Analytical Electron Microscopy for Materials Science. Kyoritsu Shuppan, 1999, p.85
5) Reimer, E.(ed.): Energy-Filtering Transmission Electron Microscopy. Springer, 1995, p.1
6) Ikematsu, Y., Shindo, D.: Materia. 40(8), 731(2001)
7) Zanchi, G. et al.: Microscopie Elecronique á Haute Tension. Proc. 4th Int. Conf. for HVEM. Toulouse, 1975, p.55
8) Castaing, R., Henry, L.: C. R. Acad. Sci. Paris, B255, 76(1962)
9) Krivanek, O. L. et al.: Microsc. Microanal. Microstruct. 2, 315(1991)
10) Shindo, D., Ikematsu, Y., Murakami, Y.: JEOL News. 35, 10(2000)
11) Egerton, R. F.: Electron Energy-Loss Spectroscopy in the Electron Microscope. 2nd ed. Plenum Press, 1996, p.434